Transport Phenomena During Freezing of Isolated Hepatocytes

Mehmet Toner and Ronald G. Tompkins
Surgical Services, Massachusetts General Hospital, Dept. of Surgery, Harvard Medical School, Boston, MA 02114

Ernest G. Cravalho
Dept. of Mechanical Engineering, Massachusetts Institute of Technology, Cambridge, MA 02139

Martin L. Yarmush
Dept. of Chemical and Biochemical Engineering, Rutgers University, Piscataway, NJ 08855

The cellular response of isolated rat hepatocytes to freezing stress under various chemical and physical conditions was investigated using cryomicroscopic observations and a theoretical transport model. Cryomicroscopy was used to determine the cellular dehydration during freezing at different cooling rates. Using these results, water permeability parameters were also obtained. In addition, intracellular ice formation (IIF) parameters were obtained from rapid freezing experiments at a cooling rate of 400°C/min to decouple the effects of dehydration from IIF. The water permeability and IIF parameters were then used in a transport model to predict the probability of IIF under a wide range of chemical and physical conditions observed during cell freezing. In order to verify the model predictions, experiments were performed under similar conditions and compared to the theoretical predictions. The results suggest that slowly cooled cells (<80°C/min) dehydrate excessively and escape IIF. On the other hand rapidly cooled cells (>120°C/min) contain enough undercooled cellular water which undergoes IIF between −5 and −12°C.

Introduction

The use of hepatocytes in a hybrid artificial liver represents a very promising approach to temporary replacement of liver function for patients with acute fulminant liver failure and/or those with chronic liver failure who are candidates for transplantation (Koshino et al., 1979; Olumide et al., 1979). However, the ultimate success of an artificial liver support device relies heavily on a readily available supply of hepatocytes. Thus, efficient and reproducible hepatocyte cryopreservation techniques are critical if an extracorporeal device is ever to become feasible. Unfortunately, efficient cryopreservation methods for hepatocytes have yet to be developed (Fuller et al., 1982; Kusano et al., 1981; Koebe et al., 1990); the primary obstacle being the lack of a fundamental understanding of the physicochemical properties governing the response of hepatocytes to freezing stress.

Correspondence concerning this article should be addressed to M. L. Yarmush or R. G. Tompkins at the Surgical Services, Massachusetts General Hospital, Bigelow 1302, Boston, MA 02114.

Injury to biological cells during a freeze-thaw cycle is related to the thermodynamic state of intracellular water (Mazur, 1984). For a cell suspension subjected to subfreezing temperatures, ice preferentially forms outside the cells in the suspending medium either due to the seeding by a chilled needle or by heterogeneous nucleation of the undercooled solution on the vessel walls. Figure 1 illustrates schematically the cellular response of cells to freezing subsequent to the seeding of extracellular ice. As a result of the formation of extracellular ice, the concentration of solutes in the external compartment increases and water efflux from the cells ensues to restore the chemical equilibrium. Based on a thermodynamic model proposed by Mazur (1963), three biophysical parameters have been shown to be important in determining the water content of the cell cytoplasm during freezing:

(1) Surface area-to-volume ratio (A/V).
(2) The hydraulic conductivity of the plasma membrane (L_{pg}).

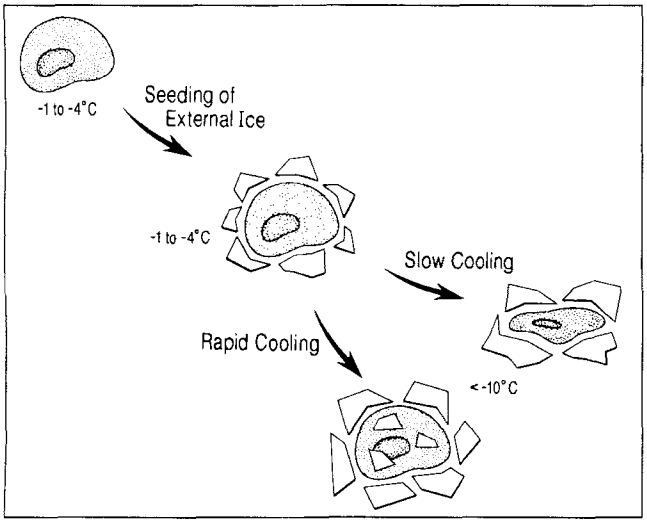

Figure 1. Schematic representation of cellular response to freezing stress.

The cell is initially cooled to a subzero temperature between −1 and −5°C and the extracellular ice is seeded by touching the suspending solution with a chilled needle. Thereafter, the cell is cooled at a given cooling rate to the storage temperature (usually below −80°C).

(3) The activation energy of the hydraulic conductivity (E_{Lp}, that is, its temperature dependence).

At slow cooling rates, the extra- and intracellular solute concentrations can be maintained nearly equal due to excessive dehydration of the cell. Cellular damage may occur by time-dependent exposure to concentrated solutions, excessive cell shrinkage, and mechanical effects of the external ice (Mazur, 1984). Conversely, at relatively fast cooling rates, heat transfer dominates over the water transport and the extracellular solute concentration increases more rapidly (due to extracellular ice formation) than can be compensated by cellular dehydration. Consequently, there is an increased likelihood that the undercooled intracellular water retained by the cells will undergo intracellular ice formation (IIF) that is lethal to cells. Then, the cooling rate which yields the maximum survival for a given cell type is usually the fastest possible cooling rate without IIF. Therefore, it is very important to be able to predict the likelihood of IIF for a given cooling protocol in addition to the prediction of the total water content of the cell. Recently, we proposed that IIF is catalyzed heterogeneously by local sites on the plasma membrane in the presence of extracellular ice (Toner et al., 1990a). According to this hypothesis, the formation of the extracellular ice alters a yet unknown local site (for example, lipids or proteins) on the plasma membrane in such a way that it becomes an efficient nucleator for ice inside the cell. The model utilizes two parameters, a kinetic parameter (Ω_o), and a thermodynamic parameter (κ_o) to describe IIF.

In the present report, we experimentally investigated the response of isolated rat hepatocytes to freezing stress using cryomicroscopy. Experimental observations were used to obtain the water permeability and intracellular ice-nucleation parameters of hepatocytes. A simple transport model which accounted for both cellular dehydration and IIF was then used to predict the cellular behavior of hepatocytes under various chemical and physical conditions during freezing. In general, satisfactory agreement was obtained between the theoretical predictions and experimental observations.

Materials and Methods

Hepatocyte isolation

The isolation techniques used to obtain isolated rat hepatocytes have been described in detail elsewhere (Dunn et al., 1989; Dunn et al., 1991). Briefly, hepatocytes were obtained from two-month old, female Lewis rats (200 g) by a modified procedure of Seglen (1973). Animals were anesthetized with ether. The liver, weighing roughly 8 g, was perfused *in situ* with 300 mL of Ca^{++}-free Krebs Ringer bicarbonate buffer, containing 5.5-mM glucose and 20-mM HEPES, pH 7.4, at 50 mL/min. The perfusate was maintained at 37°C and was equilibrated with 95% O_2 and 5% CO_2. The liver was subsequently perfused *in vivo* with 0.05% collagenase (Type IV, Sigma, St. Louis, MO) solution containing 5-mM Ca^{++} for 10 min in a recirculation system. The resulting cell suspension was filtered through two nylon meshes (Small Parts, Miami, FL), with grid sizes of 210 and 62 μm. The cell pellet was collected by centrifugation at 50 g for 5 min. Hepatocytes were further purified by a modified procedure of Kreamer et al. (1986). Briefly, the cell pellet was resuspended into 50 mL of Dulbecco's Modified Eagle Medium (DMEM, Hazelton, Lenexa, KS) and 12.5 mL of cell suspension was added to 10.8 mL of Percoll (Pharmacia, Piscataway, NJ) and 1.2 mL of 10X DMEM. The mixture was centrifuged at 500 g for 5 min, and the cell pellet was washed twice with DMEM. Routinely, 200 to 300 million cells were isolated from an 8-g liver, with viability ranging from 92–99% using trypan blue exclusion dye. The cells were resuspended in high-glucose DMEM (4.5 g/L glucose, Hazelton). All experiments were performed following a 1-h recovery period from the isolation procedure. The isolated cells were continuously held on ice until they were used for cryomicroscopic experiments. The suspending solution used for measuring the permeability coefficients was DMEM. All solutions prepared above were sterilized by filtration through a 0.22-μm filter (Nalgene, Fisher, Pittsburgh, PA).

Cryomicroscopy system

The apparatus used to cool and observe the hepatocytes, which consisted of a Zeiss Universal light microscope (Carl Zeiss, Germany), a video camera (Ikegami ITC 62, Japan), a color monitor (Panasonic S1300, Japan), a video cassette recorder (Panasonic 6300), a specially designed cryostage, a system consisting of a computer-based temperature controller and a video interface (Interface Techniques, Cambridge, MA), has been described in detail elsewhere (Cosman et al., 1989). Gaseous nitrogen, chilled by passage through a coil immersed in liquid nitrogen, was the refrigerant for the cryostage. The cryostage had a square copper base plate with an optical window in the center. The optical window (18×18 mm^2) had a 5-μm-thick foil thermocouple probe (copper-constantan, #20102, Rdf Corporation, Hudson, NH) embedded between the bottom transparent electrically conductive heating window and a top glass coverslip (Bradford Scientific, Inc., NH) for electrical insulation purposes. The lateral temperature gradient was measured across the window and determined to be less than

0.025°C/mm. Electrical power was supplied to the heating window with electrical leads attached to two gold-plated contact strips. The temperature controller provided the heating window with the power needed to counterbalance the refrigerant and thus maintained the sample at the desired temperature or set point. Computer control of the set point in time was enabled through the temperature control software. Direct correlation with time and temperature was accomplished by electronic superposition of these data on the video image. Timing signals were derived from the video chain (1/6 field rate or 0.1-s intervals) which provided the software with an accurate clock for generating the temperature protocol.

Procedures for cryomicroscopy

A 5-μL sample of the hepatocyte suspension (5×10^6 cells/mL) was placed in between the cryostage window and a cover slip (12×12 mm^2) using a microliter syringe. Silicone grease was used to seal the edges of this sandwich system to prevent evaporation of the solution during the experiments. The thickness of the sample was estimated to be between 50 and 150 μm. A 40× objective (Ph240/0.75, Carl Zeiss) and a 1.25× photo-ocular (Carl Zeiss) were used. Thermal gradients in the field of view was determined with distilled water using methods described previously (Toner et al., 1991). The maximum temperature difference recorded was 0.25°C over a field of 1 mm. Only hepatocytes located within 200 μm of the thermocouple junction were monitored to minimize errors introduced by temperature gradients across the cryostage window. The water permeability experiments were performed at constant cooling rates of 6, 50, 75, 100, 150 and 400°C/min. Each sample was initially cooled from 3°C at a constant predetermined rate to a final temperature of −40°C. Unless otherwise stated, the extracellular ice was seeded at ~ −1°C (that is, T_{seed}).

To determine the inactive cell volume, a slight variation of this method was used. Using the cryomicroscopy system, the specimen was cooled at 500°C/min from 3°C to a preset holding temperature between −1 and −5°C. The chosen preset temperature was held constant for ~2 min to make sure that an equilibrium volume was reached (~5 s). Osmolality of the specimen was estimated from the holding temperature using the relationship osm = $-T_f$(°C)/1.858.

IIF experiments were performed using similar procedures to the water transport experiments and they are described in Harris et al. (1991). Briefly, the temperature at which IIF occurred under a given freezing condition was determined from the darkening of the cell due to the light scattering from small ice crystals forming inside the cells.

Water transport model

To model the flow of water across a biological membrane, the following equation can be written from thermodynamic principles assuming that equilibria of temperature and pressure prevail between the intra- and extracellular media (Mazur, 1963; Toner et al., 1990b):

$$\frac{dV}{dT}=\frac{L_p\mathrm{ART}}{\nu_w B}\left[\ln\frac{(V-V_b)}{(V-V_b)+\nu_w(\upsilon_S n_S)}-\frac{\Delta H_f}{R}\left(\frac{1}{T_R}-\frac{1}{T}\right)\right] \quad (1)$$

where V is the cell volume; T is the absolute temperature; L_p is the water permeability; A is the surface area of the cell and is given by $(=A_o[V/V_o]^{2/3})$; A_o and V_o are the initial surface area and volume of the cells, respectively; B is the cooling rate; ν_w is the partial molar volume of water; V_b is the osmotically inactive cell volume (that is, cell solids and bound water); n_s is the number of moles of solutes in the cell as calculated from the initial osmolality (0.285 osm) and the total cell water volume $(V-V_b)$; υ_s $(=2)$ is the dissociation constant for NaCl; T_R is the equilibrium freezing temperature of pure water (273.15 K); and ΔH_f is the latent heat of fusion for water. It can be assumed in Eq. 1 that permeability is rate-limited by the passage of water through the cell membrane, and, the temperature dependence is expressed as an Arrhenius relationship (Levin et al., 1976):

$$L_p=L_{pg}\exp\left[-\frac{E_{Lp}}{R}\left(\frac{1}{T}-\frac{1}{T_R}\right)\right] \quad (2)$$

where L_{pg} is the permeability to water of the cell membrane at T_R $(=273.15$ K) and E_{Lp} is the apparent activation energy for the permeation process. Thus, a theoretical temperature-volume history of a cell during freezing can be predicted by integrating Eqs. 1 and 2 subject to the initial condition of $V=V_o$ at the temperature of extracellular ice formation (that is, T_{seed}). Extensive parameter analyses show that the solution of Eqs. 1 and 2 is most sensitive to the value of the apparent activation energy, and relatively insensitive to the value of the hydraulic water permeability (Mazur, 1963; Shabana and McGrath, 1988).

The derivation of Eq. 1 includes a number of assumptions which have been a subject of extensive research in the field of cryobiology for the past two decades (Mazur, 1963; Mansoori, 1975; Levin et al., 1979; Shabana and McGrath, 1988; Toner et al., 1990b). The effect of a linear relationship rather than a 2/3 power dependence of A upon V as in Eq. 1 has negligible (<10%) effect upon the resulting permeability parameters (Shabana and McGrath, 1988). The assumption of thermal equilibrium within the immediate vicinity of the cell is valid for cooling rates of the order of 10^4°C/min (Mansoori, 1975; Levin et al., 1979), and the temperature difference across the cell membrane during freezing is less than 0.01 K for most practical purposes (Hua et al., 1982). In Eq. 1, it was also assumed that the intracellular solution was both ideal and dilute. Although, intracellular solutions are neither ideal nor dilute, Levin et al. (1977) have shown that these effects could be easily lumped into the nonosmotic volume term V_b. It was also shown that in cases where solution nonideality and nondiluteness was included in Eq. 1, the effect upon the cell volume at subzero temperatures was negligible (Mansoori, 1975; Levin et al., 1977). Another assumption in the derivation of Eq. 1 is the zero hydrostatic pressure difference across the plasma membrane. This assumption is only valid for mammalian cells and isolated protoplasts. For plant cells, with intact cell wall, however, a turgor pressure term must be included in Eq. 1 (House, 1974; Levin et al., 1979).

Intracellular ice-nucleation model

The nucleation of ice inside biological cells during cooling in the presence of extracellular ice can be modeled using the

theory of nucleation in condensed systems (Turnbull and Fisher, 1949). In heterogeneous nucleation theory, the efficiency of a catalytic site increases with increasing numbers of water molecules oriented into an ice-like lattice (Turnbull and Vonnegut, 1950). We proposed that a local site (for example, lipids or proteins) on the plasma membrane acts as a nucleation site in the presence of extracellular ice by organizing water molecules into the critical ice-like clusters necessary to initiate ice nucleation (Toner et al., 1990a). The steady-state rate, I, of ice-like cluster formation on the surface of the nucleation catalyst can be expressed as follows (Toner et al., 1990a):

$$I = \Omega \exp[-\kappa/(\Delta T^2 T^3)] \tag{3}$$

where

$$\Omega = \Omega_o (T/T_{fo})^{1/2} (\eta_o/\eta) (A/A_o)$$

$$\kappa = \kappa_o (T_f/T_{fo})^4$$

where the subscript "o" refers to isotonic, that is, physiological conditions; Ω and κ are, respectively, the kinetic and thermodynamic parameters for heterogeneous nucleation under isotonic conditions; $\Delta T = T - T_f$ is the undercooling of the cytoplasm; T_f is the equilibrium freezing temperature of the cytoplasm; $T_{fo} = -0.52$°C for an isotonic solution of 0.285 osm/kg-H_2O; and η is the viscosity of the intracellular solution ($=0.139\ [T/225-1]^{-1.64}\ 10^{-3}$, kg/m·s). Since the crystallization time which is associated with IIF is negligible in comparison with the nucleation time, the nucleation rate for a system composed of identical biological cells can be assumed to be equivalent to the IIF crystallization rate which may be measured experimentally using a cryomicroscopic system (Harris et al., 1991). The probability of IIF can then be related to the nucleation rate by assuming sporadic nucleation of identical cells:

$$\mathcal{P} = 1 - \exp\left[-\frac{1}{B}\int_{T_{seed}}^{T} AI\,dT\right] \tag{4}$$

In Eq. 4, A and I change as a function of cellular dehydration during freezing which can be predicted using Eq. 1. The effects of various assumptions and parameters in Eqs. 3 and 4 have been investigated in detail in Toner et al. (1990a). In summary, the thermodynamic state of the intracellular solution can be characterized using a set of water transport (L_{pg} and E_{Lp}) and ice-nucleation (Ω_o and κ_o) parameters which can be measured using cryomicroscopy.

Data analysis and statistics

Following each experiment, the video recordings were analyzed to determine the volume variation of each hepatocyte. The method used to analyze images for water permeability experiments was semiautomatic. The computer placed the video recorder in the playback freeze-frame mode and superimposed a cursor on the image. Using a mouse, the cursor was moved to the cell boundary on the image, and points were plotted around the periphery of the cell. The enclosed area was then computed using a polygonal approximation and was related to the cell volume by assuming spherical geometry. For each different cooling rate investigated, cell volumes were obtained from two to three different hepatocyte isolation examining two to five cells per isolation. The mean ±SDM of the volumes were calculated from the pooled data at a given subzero temperature with 1°C increments.

Nonlinear regression analysis was used to obtain values for the permeability values that would produce the *best fit* between experimental volume measurements and theoretical volumes predicted by the model (that is, Eq. 1) as described in detail elsewhere (Levin et al., 1979). Briefly, the applied fitting technique minimized the difference between the theoretical and experimental volume curves as judged by the variance or value of the chi-squared statistics, χ^2 (Bevington, 1959). Two different methods were used to minimize χ^2. The gradient search method was employed for conditions far from convergence, and the linearization method was applied for conditions near convergence. Values of L_{pg} and E_{Lp} were adjusted by iteration until the change in χ^2 between successive iterations converges to $\Delta\chi^2/\chi^2 < 0.01$. The predicted permeability coefficients at different cooling rates for rat hepatocytes were then averaged to obtain a universal set of permeability coefficients. The model predictions using this universal set of permeability coefficients were compared with experimental measurements using the two-sample Wilcoxon signed rank test at a significance level of $\alpha = 0.05$ (Kennedy and Neville, 1974). Similar data analysis and curve-fitting methods were also used for ice-nucleation parameters (that is, Eq. 10).

Results

Water permeability parameters

The estimation of water permeability coefficients, L_{pg} and E_{Lp}, from the measured volumetric response requires independent estimation of the initial cell diameter and inactive cell volume (that is, cell solids and bound water). A mean ●SDM diameter of 21.2±2 μm was determined from the average projected area of ninety-one isolated hepatocytes at ambient temperature in DMEM. Figure 2 shows the experimental diameter distribution of isolated rat hepatocytes which can be used to predict the initial cell volume and surface area. The inactive cell volume was predicted from the equilibrium osmometric behavior at different subzero temperatures between −1 and −6°C in the presence of extracellular ice. The osmolality of the external partially frozen solution is given by the relation osm = $-T_f$(°C)/1.858. Hepatocyte volume decreased rapidly within a few seconds (Figure 3) indicating a rapid re-equilibration with the partially frozen external solution. The volume measurement was recorded at the end of ~2 min to ensure that complete equilibration had occurred. Regression analysis of data obtained at various temperatures between −1 and −6°C yielded the Boyle-van't Hoff function of $V/V_o = 0.51 + 0.14/\text{osm}$ as shown in Figure 4. The osmotically inactive fractional cell volume can be estimated to be 0.51 by extrapolation to an infinitely concentrated solution.

In order to determine the water permeability parameters, cryomicroscopic measurements of cell volume as a function of temperature at different cooling rates were performed. Figure 5 depicts a micrograph showing the response of three isolated hepatocytes during freezing at a cooling rate of 100°C/min. As can be seen from this figure, two of the hepatocytes

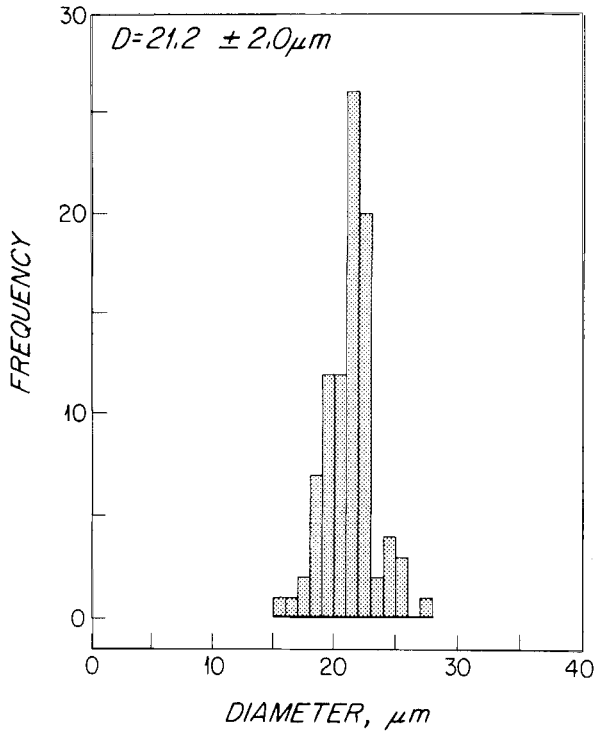

Figure 2. Diameter (D) distribution of isolated rat hepatocytes in DMEM at 22°C.

The mean diameter ±SDM is 21.2±2μm ($n=91$).

dehydrated excessively prior to reaching −8°C while the third one formed intracellular ice as evident from the darkening of the cell. For cooling rates between 6 and 100°C/min, cells exhibited little appreciable volume change below −8°C indicating excessive dehydration prior to reaching −8°C. For cooling rates of 150 and 400°C/min, hepatocytes formed

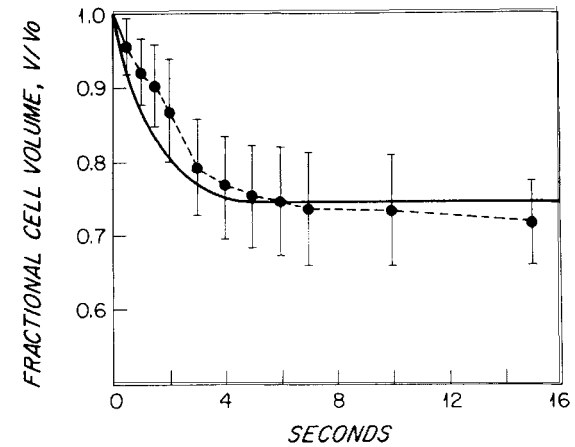

Figure 3. Volumetric behavior of isolated rat hepatocytes as a function of time at a constant holding temperature of −1.1°C in the presence of extracellular ice.

Solid line represents the theoretical prediction using the water permeability parameters obtained in Figure 5. Error bars represent standard deviations of the mean. Seven hepatocytes were used in these experiments.

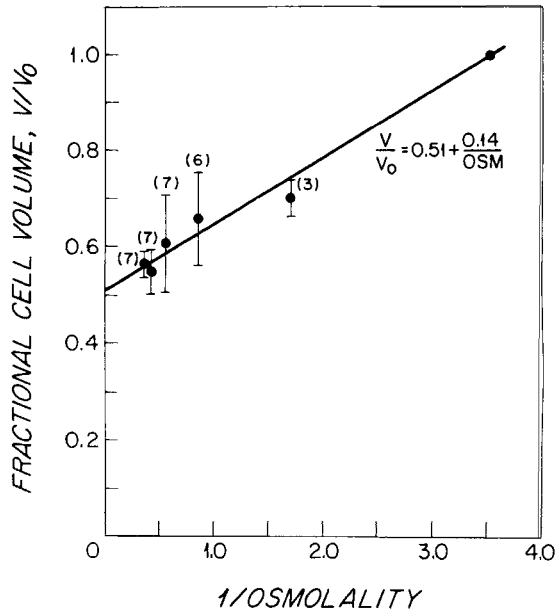

Figure 4. Static osmometric behavior measured at constant subzero temperatures in the presence of external ice for isolated rat hepatocytes in DMEM.

The number in parentheses represents the number of hepatocytes used for each data point. Error bars represent standard deviations of the mean. The holding temperature was related to the osmolality by the relation osm = $-T_f(°C)/1.858$. Linear regression was used to determine the Boyle-van't Hoff function given in this figure.

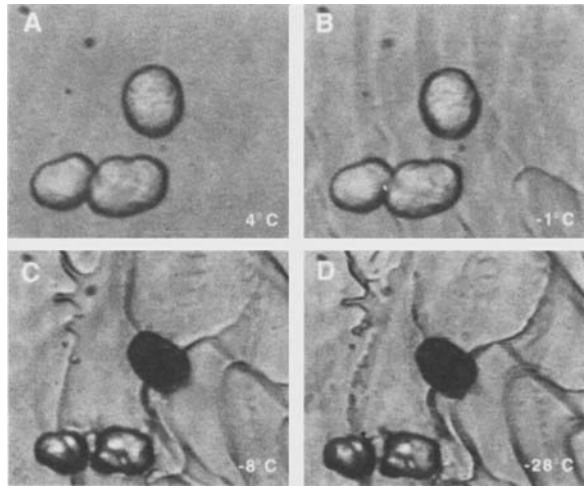

Figure 5. Micrograph of three isolated hepatocytes during freezing at a cooling rate of 100°C/min: (A) Prior to freezing at 4°C; (B) freezing starts at −1°C with the formation of external ice; (C) two of the hepatocytes are dehydrated whereas one of them formed internal ice at −8°C (the darkening of one of the hepatocytes is caused by the formation of intracellular ice); (D) hepatocytes at −20°C.

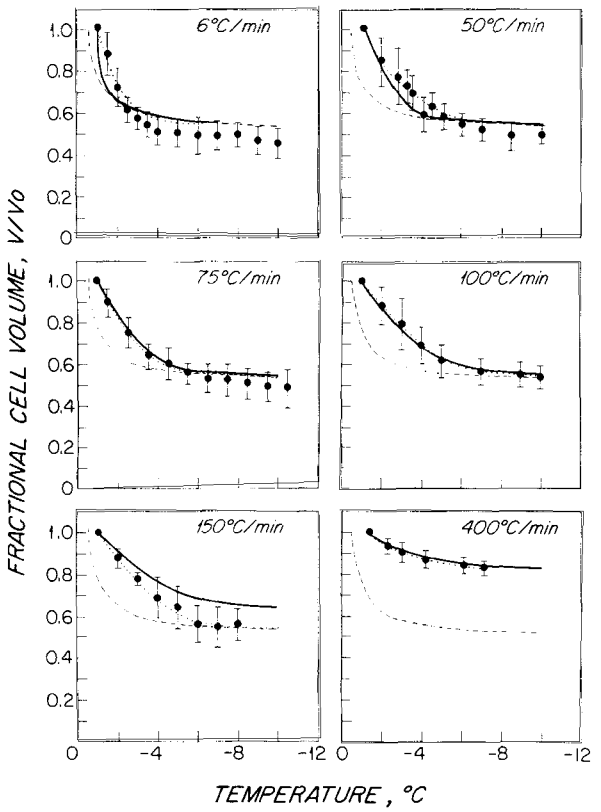

Figure 6. Changes in volume of isolated rat hepatocytes as a function of temperature for different cooling rates.

Experimental points (circles) represent an average of 5 to 16 cells from 2 to 4 independent experiments. Bars represent the standard deviation of the mean. Theoretical curve-fits (dotted lines) yielding the best value of the permeability coefficients given in Table 1 are also shown at each cooling rate. Theoretical predictions (solid lines) were performed using mean values of the water permeability coefficients (that is, $L_{pg}=(1.5\pm0.9)\times10^{-12}$ m^3/N·s and $E_{Lp}=341.1\pm70.1$ kJ/mol). The dashed lines represent the equilibrium freezing curve when the cell are cooled infinitely slowly. This curve is obtained from Eq. 1 for $dV/dT=0$.

intracellular ice at ~ −8°C preventing further cell dehydration and data analysis. Thus, the permeability coefficients were determined between ~0 and −8°C as shown in Figure 6. Variations in fractional volume could be attributed to permeability differences between individual cells, to limitation involving the use of two-dimensional information, and/or an assumption of perfect spherical geometry. Experimentally determined volume changes were correlated with Eq. 1 using the inverse curve-fitting method described above to yield permeability coefficients at six different cooling rates between 6 and 400°C/min (Table 1).

To assure that a single set of permeability coefficients could be used to reasonably describe the dehydration behavior of hepatocytes, a mean water permeability coefficient for all the cooling rates considered in this study was calculated from the values listed in Table 1. Using mean values, $L_{pg}=(1.5\pm0.9)$ 10^{-12}m^3/N·s and $E_{Lp}=341.1\pm70.1$ kJ/mol, volumetric behavior predictions (solid lines) were superimposed on the experimental measurements in Figure 6. The experimental observations were not statistically significantly different than the predictions obtained by using the mean permeability coefficients for cooling rates studied in this investigation as assessed by the two-sample Wilcoxon signed rank test. These data suggest that the dehydration behavior of isolated rat hepatocytes could be adequately described using a single set of permeability coefficients over a wide range of cooling rates between 6 and 400°C/min.

Table 1. Water Permeability of Isolated Hepatocytes at Subzero Temperatures as a Function of Cooling Rate in the Presence of External Ice

Cooling Rate, B (°C/min)	L_{pg} (10^{+12}m^3/N·s)	E_{Lp} (kJ/mol)	Variance* ($\times10^{+3}$)	No. of Cells
6	0.3	322.3	1.9	8
50	0.9	327.3	0.4	7
75	2.4	424.9	0.2	16
100	1.1	268.7	0.1	7
150	1.8	275.4	0.3	9
400	2.7	427.8	0.1	5

*The variance of the fit is characterized by the statistic χ^2 defined as the sum of square of residuals (Bevington, 1959).

Ice nucleation parameters

In order to investigate ice nucleation with as little interference of dehydration, experiments to observe the kinetics of IIF were performed at a rapid cooling rate (400°C/min). Heterogeneous nucleation theory was used to estimate the ice nucleation parameters for hepatocytes. Experimentally determined kinetics of IIF (Figure 7) were correlated with Eqs. 3

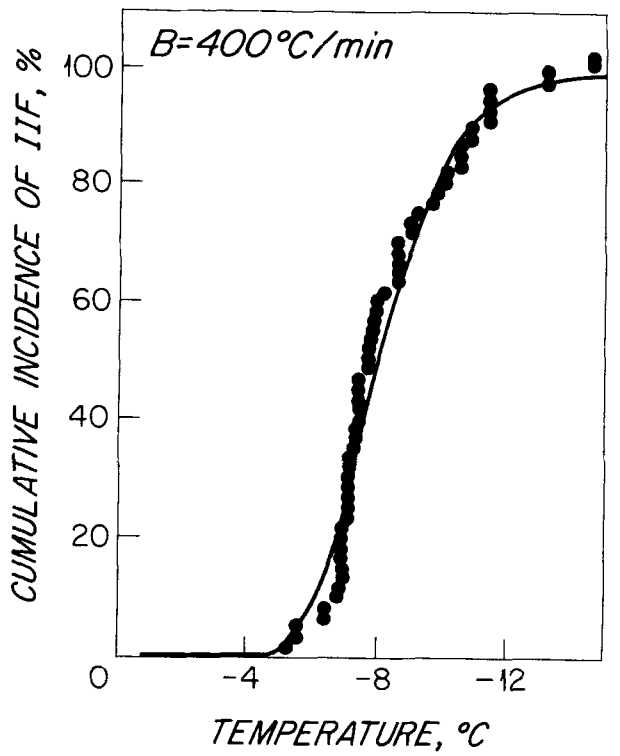

Figure 7. Temperature dependence of the cumulative incidence of isolated rat hepatocytes with intracellular ice.

The cooling rate is 400°C/min in DMEM. Nonlinear regression analysis is used to obtain best fit to experimental data points. Table 2 depicts the values of ice nucleation parameters. Experimental results are discussed in detail in Harris et al. (1991).

Table 2. Ice Nucleation Parameters of Isolated Rat Hepatocytes Cooled at Constant Rates in the Presence of Extracellular Ice

Cooling Rate, B (°C/min)	$\Omega_o \times 10^{-10}$ $(m^2 \cdot s)^{-1}$*	$\kappa_o \times 10^{-9}$ (K^5)*	Variance** ($\times 10^3$)
400	1.1	1.4	3.9
150	1.2	1.5	2.5
125	0.4	1.4	6.1
100	1.0	2.6	7.6
75	1.0	1.5	2.7

*The mean value of the ice nucleation parameters were determined from the above table to be (mean ± SDM)$\Omega_o = (0.9 \pm 0.3) \times 10^{10}$ $(m^2 \cdot s)^{-1}$ and $\kappa_o = (1.7 \pm 0.5) \times 10^9$ (K^5).
**The variance of the fit is characterized by the statistic χ^2 defined as the sum of square of residuals.

to 4 using the inverse curve-fitting technique described in Materials and Methods. The fitted values for the nucleation parameters were $\Omega_o = 1.1 \times 10^{10} (m^2 \cdot s)^{-2}$ and $\kappa_o = 1.4 \times 10^9$ K^5. Theoretical prediction of the variation in IIF with temperature using the fitted nucleation parameters is shown in Figure 7 together with the experimental observations at 400°C/min. Variance of the theory and experiment is less than 4.0×10^{-4} indicating a good curve-fit.

To verify the ice nucleation parameters obtained from IIF experiments at 400°C/min, we have also determined the ice nucleation parameters at slow cooling rates by coupling the water transport to the cumulative incidence of IIF. Experimental data for this analysis is published in detail elsewhere (Harris et al., 1991). Results of these calculations are shown in Table 2. The values obtained at various cooling rates were not statistically different from each other with mean values (mean ± SDM) of $\Omega_o = (0.9 \pm 0.3) \times 10^{10} (m^2 \cdot s)^{-1}$ and $\kappa_o = (1.7 \pm 0.5) \times 10^9$ K^5. Thus the ice nucleation parameters obtained at a rapid cooling rate (400°C/min) can be used to describe the IIF behavior at other cooling rates.

Prediction of intracellular ice formation

Given the experimental data obtained, the theory presented in the Materials and Methods section can now be applied to the prediction of IIF of isolated rat hepatocytes under various freezing conditions. Since it is known that IIF correlates with lethal injury to cells, it is especially important to know the critical cooling rate range over which the likelihood of IIF increases from 0% to 100%. The maximum cumulative incidence of IIF in isolated rat hepatocytes during cooling to a temperature of −40°C at constant cooling rates in physiological media is predicted as shown in Figure 8 (solid line). The maximum cumulative incidence of IIF as predicted from Eqs. 1 to 4 increases from 0% at approximately 80°C/min to 100% at approximately 120°C/min. Experimental results from hepatocytes cooled under similar conditions are also depicted in Figure 8 showing a reasonable agreement between model predictions and experiments.

It is also important to determine the temperature at which IIF occurs as a function of cooling rate to be able to design freezing protocols without IIF. The model is used to predict the average temperature at which 50% of cells undergo IIF ($^{50}T_{IIF} \pm$SDM) yielding -9.3 ± 0.8°C between 75 and 400°C/min as shown in Figure 9. Theoretical results suggest that $^{50}T_{IIF}$

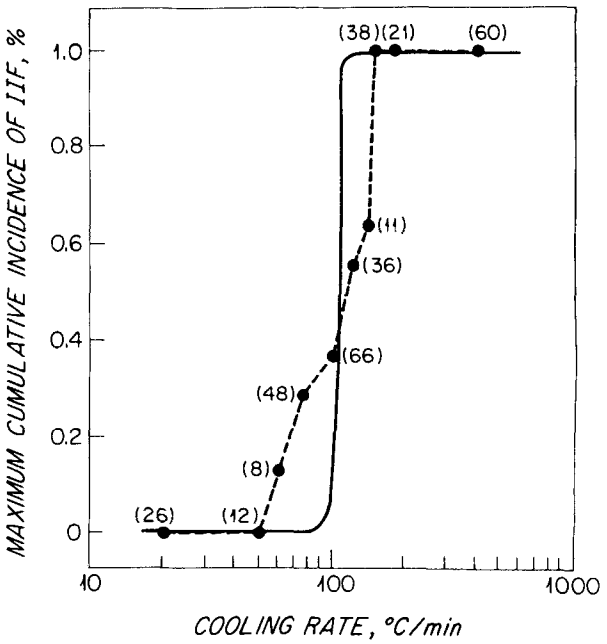

Figure 8. Model prediction of the effect of cooling rate on the maximum cumulative incidence of IIF isolated rat hepatocytes.

The solid line is the model prediction and the circles are experimental observations from Harris et al. (1991). The number of hepatocytes observed at each cooling rate is shown. Results are pooled from 2 to 6 experiments with 4 to 15 hepatocytes per experiment.

is relatively insensitive to the cooling rate. Experimental $^{50}T_{IIF} \pm$SDM for isolated hepatocytes is also insensitive to the cooling rate with a mean value of -7.7 ± 0.7°C and is in agreement with theoretical predictions.

In order to minimize the damage to cells, it is preferred to dehydrate the cells at the lowest possible temperature without

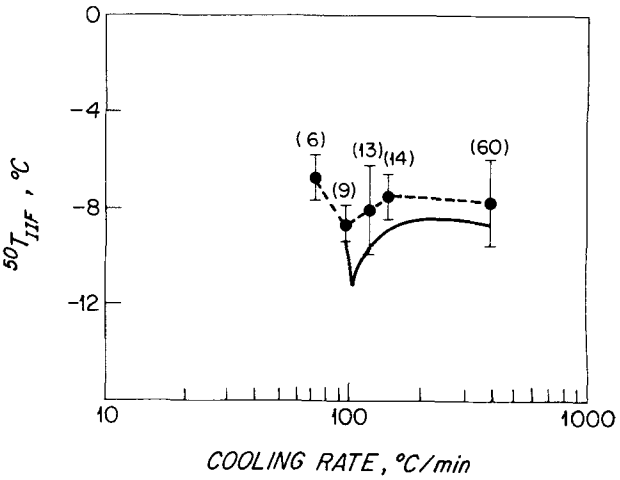

Figure 9. Model prediction of the effect of the cooling rate on $^{50}T_{IIF}$ for isolated rat hepatocytes.

The solid line is the model prediction and circles are experimental observations from Harris et al. (1991). The number of hepatocytes observed at each cooling rate is shown. Results are pooled from 2 to 6 experiments with 4 to 15 hepatocytes per experiment. Bars represent standard error of the mean.

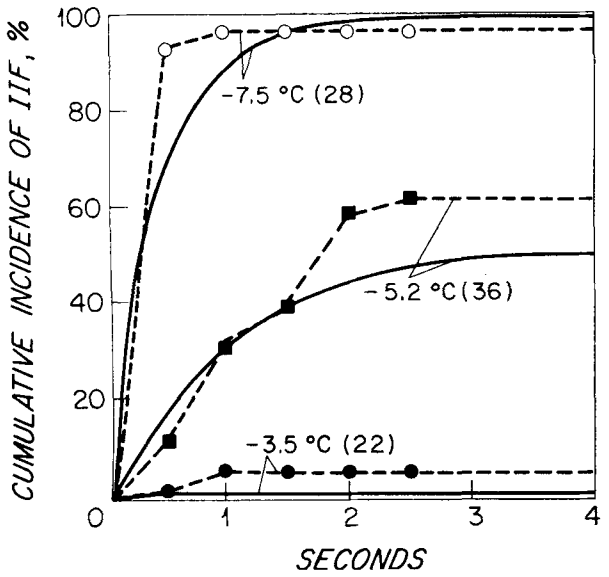

Figure 10. Model prediction of the cumulative incidence of IIF as a function of time at constant holding temperatures.

The solid lines are model predictions and the symbols are experimental observations from Harris et al. (1991). The number of hepatocytes at each temperature is shown in parentheses.

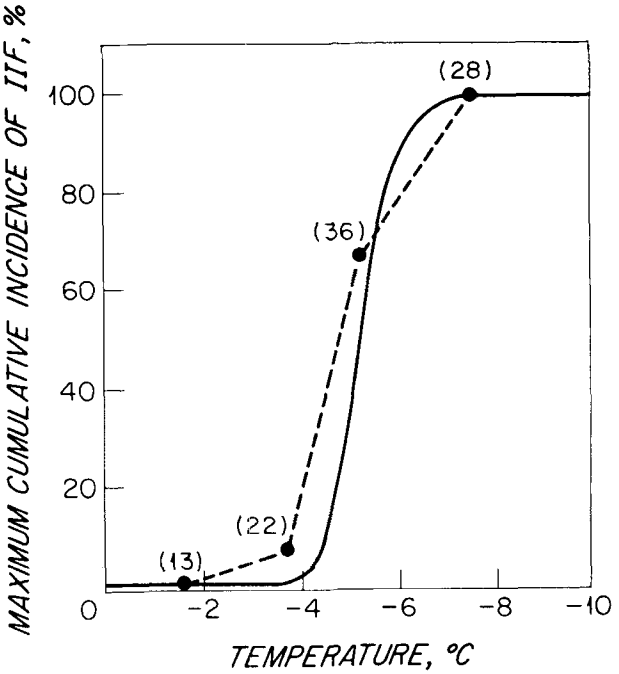

Figure 11. Model prediction of the temperature dependence of the maximum cumulative incidence of IIF under isothermal conditions.

The solid lines are model predictions and circles are experimental observations from Harris et al. (1991). The number of hepatocytes at each temperature is given.

IIF. Thus the time dependence of IIF at different constant temperatures needs to be investigated. The predicted cumulative incidences of IIF during isothermal holding periods at several temperatures are shown in Figure 10. The cumulative incidence of IIF increases continually with time during an isothermal holding period. In addition, the rate of IIF is faster at lower temperatures. For a holding temperature of $-7.5°C$, it takes ~ 1 sec to reach the maximum cumulative incidence of IIF of 100%. At $-5.2°C$, a maximum cumulative incidence of IIF of $\sim 50\%$ is reached in ~ 2 s. Hepatocytes that do not show IIF during the first ~ 2 s remain unfrozen because they reach thermodynamic equilibrium with the external ice by dehydration. The maximum cumulative incidence of IIF as a function of various isothermal holding temperatures in the presence of external ice is plotted in Figure 11. According to both theory and experiment, the maximum cumulative incidence of IIF increases from 0 at $\sim -3°C$ to 100% at $\sim -7.5°C$. The ${}^{50}T_{IIF}$ obtained from isothermal holding conditions (that is, $\sim -5.2°C$) is significantly higher than ${}^{50}T_{IIF}$ observed under continuous cooling rates (that is, $\sim -9.3°C$). This difference is because IIF is a function of time and temperature, and even at a constant temperature there will be a certain portion of cells which will continue to develop IIF. The proposed model accounts for both the time and temperature dependence of IIF quantitatively.

All aforementioned theoretical predictions assume that external ice is seeded at $T_{seed} \sim -1°C$ by touching with a chilled needle. Since the water content of cells during cooling will also depend on the temperature at which external ice is seeded (that is, dehydration starts due to increased extracellular solute concentration), it is important to be able to predict the effect of T_{seed} on IIF. Figure 12 depicts the effect of the value of T_{seed} on the maximum cumulative incidence of IIF as a function of different cooling rates. As can be seen from this figure, the

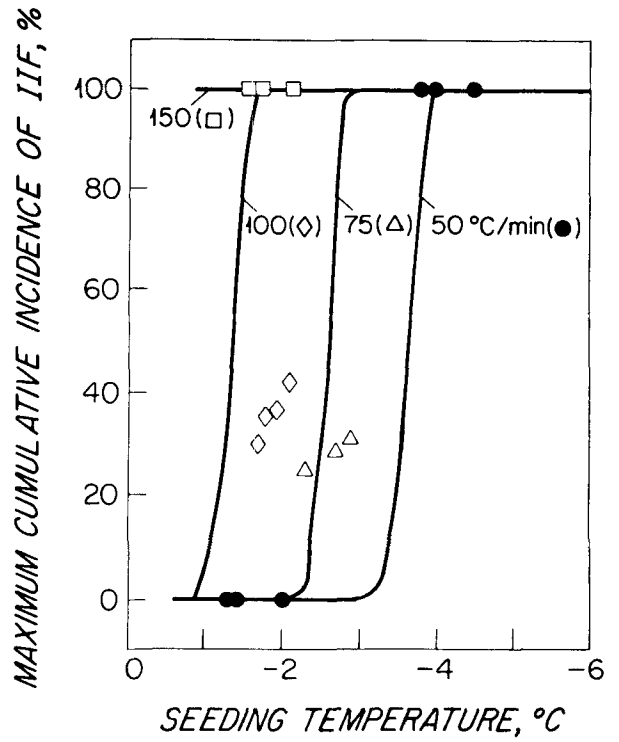

Figure 12. Prediction of the extracellular ice seeding temperature dependence of the maximum cumulative incidence of IIF as a function of cooling rate for isolated rat hepatocytes.

Lines are model predictions and symbols are experimental observations.

maximum cumulative incidence of IIF increases with decreasing T_{seed}. For lower values of T_{seed}, there will be less time for the cell to dehydrate so that the volume of water within the cell at any subzero temperature will be greater, thus increasing the likelihood of IIF. In addition, it can be seen from Figure 12 that the maximum cumulative incidence of IIF increases with increasing cooling rate for a given T_{seed}. This is because more water is retained in the cell at higher cooling rates at any subzero temperatures. Although the experimental correlation shown in Figure 12 is quantitatively poor, the results qualitatively support the theoretical dependence of the IIF behavior on the T_{seed}.

Discussion

The cellular response of isolated rat hepatocytes to freezing stress under different conditions was evaluated using cryomicroscopy and a coupled water transport and ice-nucleation model. Experimental observations of cellular dehydration were used to estimate the water permeability parameters of hepatocytes at subzero temperatures. IIF parameters were also obtained from cryomicroscopic investigation of hepatocytes at a rapid enough cooling rate (400°C/min) to minimize cellular dehydration. In this way, we were able to decouple the cellular dehydration from IIF kinetics and investigate them separately. These parameters, determined from a limited number of experimental observations, were then used in a coupled transport model to predict the response of hepatocytes to various chemical and physical conditions during freezing. Satisfactory agreement between theoretical predictions and experimental observations for a wide range of conditions supports the validity of the proposed model and its underlying assumptions.

Water transport

The calculated L_{pg} value of 1.5×10^{-12} m^3/N·s for isolated hepatocytes in the current work is much higher than that previously reported for other cells (see McGrath, 1988, for a comprehensive review). The only reported value that is higher than our value for isolated hepatocytes is that of erythrocytes ($\sim2\times10^{-12}$ m^3/N·s) (Rich et al., 1968). Similarly, the E_{Lp} value of 341.1 kJ/mol appears high when compared to other cell types. Since the activation energy for the self-diffusion of water is ~16.7 kJ/mol. This high *apparent* activation energy indicates unfacilitated, passive transport of water molecules that is probably through the lipid phase of the membrane. The main resistance to diffusion of water across a membrane will be offered by either the solution-membrane interfaces (absorption rate-limited) or by the bulk portion (diffusion rate-limited) of the membrane (Levin et al., 1976). The discrimination between these two mechanisms is possible only after the dependence of the membrane permeability on the partition coefficient and membrane thickness is determined. Unfortunately, this determination is extremely difficult, if not impossible, for water permeation through natural membranes. Therefore, the present evidence does not allow us to relate the apparent activation energy to a specific mechanism of transport across the membrane. It is unlikely that the experimental uncertainties (that is, projected area to volume transformations, cell perimeter tracings) could account for the high values of the permeability parameters since similar methods have been used in our laboratory for other cell types with reasonable predictions (Toner et al., 1989; Toner et al., 1990b). Another possible reason for the high values for E_{Lp} could involve subzero membrane damage which presumably would result in salt transport (countercurrent to the water transport) from outside to inside the cell. However, this possibility is unlikely because of several reasons. First, the good correlation between the water permeability model predictions and experimental observations over a wide range of cooling rates between 6 and 400°C/min suggests that the plasma membrane remained intact. Secondly, the equilibrium behavior determined at subzero temperatures in the presence of extracellular ice showed perfect osmometric behavior ($r^2=0.995$) further suggesting that the membrane integrity was not compromised during freezing (that is, Figures 3 and 4).

Intracellular ice-nucleation

The critical thermodynamic states which result in IIF can be predicted using the model described in this article. A major assumption in the model described in this study is that a local site (yet unknown) on the plasma membrane becomes an active ice nucleator due to the interaction with extracellular ice. The exact nature of this interaction between the external ice and the plasma membrane remains unknown. The nature of this interaction could be chemical, electrical, mechanical, ionic, and thermal or a some combination of these phenomena. It should be pointed out that some of these effects of the external ice on cells are difficult to separate from one another.

Qualitatively, the catalytic activity of an ice-nucleating surface can be characterized by the contact angle, θ, between the surface and the microscopic ice nucleus. The value of the contact angle can be estimated from κ_o as follows:

$$\kappa_o = 16\pi(\sigma^{\alpha\beta})^3 T_{fo}^4 f(\theta)/(3k\Delta H_f^2) \qquad (5)$$

where v^α and v^β are, respectively, the molecular volume of water and ice; $\sigma^{\alpha\beta}$ is the ice-liquid surface free energy; $f(\theta)$ is the heterogeneous nucleation factor. Assuming that the catalytic surface is much larger in size than the critical microscopic ice-nucleus, $f(\theta)$ can be estimated from ice-like clusters having the form of spherical sectors on a flat surface:

$$f(\theta) = (1-\cos\theta)^2(2+\cos\theta)/4 \qquad 0\le f(\theta)\le 1 \qquad (6)$$

Further insight into the possible role of membrane in IIF can be obtained from the value of the contact angle, θ. The contact angle θ is estimated to be ~19° from Eqs. 5 and 6 using the value 1.39×10^9 K^5 for κ_o and a value of 22×10^{-3} J/m^2 for $\sigma^{\alpha\beta}$. The cap radius, a, of the cluster, which is the size of the active ice nucleating site on the membrane, can also be calculated from the value of θ if the radius of the critical cluster is known (Uhlmann and Chalmers, 1965). The cluster radius can be estimated from the thermodynamic barrier to ice nucleation as $r^* = -2\sigma^{\alpha\beta}T_f^2/(\Delta H_f \Delta TT)$. This calculation yields a critical ice-like cluster radius of ~5.1 nm for hepatocytes. Therefore, the cap radius, $a = r^* \sin\theta$, is ~1.7 nm for hepatocytes. This value for the cap radius is comparable to the size of membrane proteins and lipids (Kotyk et al., 1988). Although these simple calculations do not provide any direct evidence, it is plausible that IIF is catalyzed by the protein or lipid

components of the plasma membrane which change their configuration and become good ice nucleators via the effects of the extracellular ice.

Effects of various freezing conditions on IIF and comparison with other cell types

Using the biophysical parameters determined from cryomicroscopic observations, the transport model of cell volume regulation and the likelihood of IIF outlined above was employed to determine the effects of various experimental parameters on IIF. The likelihood of IIF shows strong dependence on the cooling rate (Figure 8). Hepatocytes dehydrate for cooling rates slower than 100°C/min and escape IIF. On the other hand, for cooling rates faster than 100°C/min, hepatocytes do not have enough time to sufficiently dehydrate and the remaining intracellular water reaches thermodynamic equilibrium with the external partially frozen solution by a phase change from the liquid to the crystalline state. The existence of a cell-specific transition zone between slow and high cooling rates is consistent with observations from other cell types (Mazur, 1984; Hubel et al., 1991; Yarmush et al., 1991). For example, the *transition zone* for mouse oocytes has been determined to be between 0 and 1°C/min both from the theory and experiments (Toner et al., 1991; Toner et al., 1992). The two orders-of-magnitude difference in the critical cooling rate between hepatocytes and oocytes may be attributed to the differences in their water permeability and ice nucleation parameters.

One interesting observation is the insensitivity of the temperature of IIF to the cooling rate (Figure 9). This insensitivity of ${}^{50}T_{IIF}$ to the cooling rate has been shown for many other cell types in the absence of cryoprotective agents (Morris and McGrath, 1981; Callow and McGrath, 1985; Scheiwe and Korber, 1987; Shabana and McGrath, 1988; Muldrew and McGann, 1990; Toner et al., 1992; Pitt et al., 1991; Hubel et al., 1991). Although the cooling rate dependence of ${}^{50}T_{IIF}$ is negligible, the theoretical and experimental observations show a noticeable depression which occurs at ~108°C/min (at the *transition zone* when the cumulative incidence of IIF increases from 0 to 100%). A similar minimum for ${}^{50}T_{IIF}$ at the *transition zone* for a cooling rate of 1.8°C/min has also been observed in our mouse oocyte studies both theoretically and experimentally (Toner et al., 1991). Similar depressions in ${}^{50}T_{IIF}$ have been observed experimentally in other cell types (Morris and McGrath, 1981; Shabana and McGrath, 1988; Pitt et al., 1991).

The time dependence of IIF can be investigated by exposing the cells to different constant temperatures in the presence of extracellular ice. At a constant subzero temperature, cells will dehydrate due to the osmotic force generated by the formation of the extracellular ice while a certain portion of cells undergo IIF by the surface catalyzed mechanism suggested in this study. The fraction of cells with IIF is a function of temperature, lower temperatures yielding a higher fraction of cells with IIF. The ${}^{50}T_{IIF}$ obtained from isothermal holding conditions (that is, ~ −5.2°C) depicted in Figure 11 is significantly higher than ${}^{50}T_{IIF}$ observed under continuous cooling rates (that is, ~ −9.3°C) shown in Figure 7. This difference is because IIF is a function of time and temperature, and even at a constant temperature there will be a certain portion of cells which will continue to develop IIF. The results for IIF at constant holding temperature is consistent with similar results obtained for mouse oocytes (Toner et al., 1991) and *Drosophila melanogaster* embryos (Pitt et al., 1991).

Another important parameter that needs to be precisely controlled during cryopreservation of cells is the temperature at which extracellular ice is seeded. Both theoretical and experimental observations from this study show that lower seeding temperatures at a given cooling rate result in higher fraction of cells with IIF. This is because for lower values of T_{seed} there is less time for the cell to dehydrate. Thus, the volume of water within the cell at any temperature is greater which in turn leads to a higher incidence of IIF (Figure 12). Predictions from this study are also qualitatively similar to experimental observations using red blood cells (Diller, 1975) and granulocytes (Schwartz and Diller, 1984) and theoretical predictions for mouse oocytes (Toner et al., 1992).

In summary, the coupled transport model for cell volume regulation and intracellular ice-nucleation can be successfully used to predict the critical thermodynamic states which induce IIF in isolated rat hepatocytes. Ultimately, this model and further understanding of the response of hepatocytes to freezing stress can be used to design optimal cryopreservation protocols. The model can also be used to characterize the cellular response of hepatocytes to vascular freezing during cryosurgery (Rubinsky and Pegg, 1988).

Acknowledgment

We are indebted to Mrs. C. Harris and Dr. A. Hubel for the critical reading of an earlier version of this manuscript. The authors are grateful to L.M. Sterling for her technical support throughout this research. This research is supported in part by The Whitaker Foundation, Mechanicsburg, PA, and the Shriners Burns Institute, Boston, MA.

Notation

A = surface area of the cell (m^2)
a_w = water activity
B = cooling rate (°C/min)
E_{Lp} = activation energy of the water permeability (J/mol)
ΔH_f = latent heat of fusion (J/m^3 or J/mol)
I = nucleation rate per surface area ($1/m^2 \cdot s$)
L_p = water permeability ($m^3/N \cdot s$)
L_{pg} = water permeability at T_R ($m^3/N \cdot s$)
n = number of moles
N^S = number of water molecules in contact with the catalytic site
$\mathcal{P}$ = probability of intracellular ice formation
r = radius of ice cluster (m)
R = universal gas constant ($J/m^3 \cdot K$ or $J/mol \cdot K$)
T = absolute temperature (K)
T_f = equilibrium freezing temperature (K)
T_R = reference temperature (K)
x = mole fraction
v_s = dissociation constant for NaCl
V = cell volume (m^3)

Greek letters

η = viscosity ($kg \cdot m/s$)
θ = contact angle (°)
κ = thermodynamic parameter for ice-nucleation (K^5)
ν = partial molar volume (m^3/mol)
σ = surface free energy (J/m^2)
Ω = kinetic parameter for ice-nucleation ($1/m^2 \cdot s$)

Superscripts

ex = extracellular
in = intracellular

α = liquid (water) phase
β = solid (ice) phase
* = critical-size cluster

Subscripts

o = isotonic
s = solute
seed = seeding of external ice
w = water

Literature Cited

Bevington, P. R., *Data Reduction and the Error Analysis for the Physical Sciences*, McGraw-Hill, New York, p. 204-246 (1959).

Callow, R. A., and J. J. McGrath, "Thermodynamic Modelling and Cryomicroscopy of Cell-sized, Unilamellar, and Paucilamellar Liposomes," *Cryobiol.*, **22**, 251 (1985).

Cosman, M. D., M. Toner, J. Kandel, and E. G. Cravalho, "An Integrated Cryomicroscopy System," *Cryo-Letters* **10**, 17 (1989).

Diller, K. R., "Intracellular Freezing: Effect of Extracellular Supercooling," *Cryobiol.*, **12**, 480 (1975).

Dunn, J. C. Y., M. L. Yarmush, H. G. Koebe, and R. G. Tompkins, "Hepatocyte Function and Extracellular Matrix Geometry: Long-Term Culture in a Sandwich Configuration," *FASEB J.*, **3**, 174 (1989).

Dunn, J. C. Y., R. G. Tompkins, and M. L. Yarmush, "Long-Term Function of Hepatocytes Sandwiched between Two Collagen Layers," *Biotech. Prog.*, **7**, 237 (1991).

Fuller, B. J., B. W. Grout, and R. J. Woods, "Biochemical and Ultrastructural Examination of Cryopreserved Hepatocytes in Rats," *Cryobiol.*, **19**, 493 (1982).

Harris, C. L., M. Toner, A. Hubel, E. G. Cravalho, M. L. Yarmush, and R. G. Tompkins, "Cryopreservation of Isolated Hepatocytes: Intracellular Ice Formation under Various Chemical and Physical Conditions," *Cryobiol.*, **28**, 436 (1991).

House, C. R., *Water Transport in Cells and Tissue*, Williams & Wilkins, Baltimore (1974).

Hua, T. C., E. G. Cravalho, and L. Jiang, "The Temperature Difference across the Cell Membrane during Freezing and its Effect on Water Transport," *Cryo-Letters*, **3**, 255 (1982).

Hubel, A., M. Toner, E. G. Cravalho, M. L. Yarmush, and R. G. Tompkins, "Intracellular Ice Formation during Freezing of Hepatocytes Cultured in a Double Gel Collagen Gel," *Biotech. Prog.*, **7**, 554 (1991).

Kennedy, J. B., and A. M. Neville, *Basic Statistical Methods for Engineers and Scientists*, 2nd Edition, Harper and Row, New York, p. 218-219 (1974).

Koebe, H. G., J. C. Y. Dunn, M. Toner, L. M. Sterling, A. Hubel, E. G. Cravalho, M. L. Yarmush, and R. G. Tompkins, "A New Approach to the Cryopreservation of Hepatocytes in a Sandwich Culture Configuration," *Cryobiol.*, **27**, 576 (1990).

Koshino, I., H. Sakamoto, Y. Shinada, Y. Tsuji, T. Kawamata, M. Matsushita, R. Kno, and Y. Kasai, "Use of Liver Slices for an Artificial Liver," *Trans. Amer. Soc. Artif. Intern. Organs*, **25**, 493 (1979).

Kotyk, A., K. Janacek, and J. Koryta, *Biophysical Chemistry of Membrane Functions*, John Wiley & Sons, New York (1988).

Kreamer, B. L., J. L. Staecker, N. Sawada, G. L. Sattler, M. T. Hsia, and H. C. Pitot, "Use of Low-Speed, Iso-Density Percoll Centrifugation Method to Increase the Viability of Isolated Rat Hepatocytes Preparation," *In Vitro Cell. Dev. Biol.*, **22**, pp. 201-211 (1986).

Kusano, M., H. Ebata, T. Onishi, T. Saito, and M. Mito, "Transplantation of Cryopreserved Isolated Hepatocytes into the Rat Spleen," *Transplant. Proc.*, **13**, 848 (1981).

Levin, R. L., E. G. Cravalho, and C. E. Huggins, "A Membrane Model Describing the Effect of Temperature on the Water Conductivity of Erythrocyte Membranes at Subzero Temperatures," *Cryobiol.*, **13**, 419 (1976).

Levin, R. L., E. G. Cravalho, and C. E. Huggins, "The Effect of Solution Non-Ideality on RBC Volume Regulation," *Biochim. Biophys. Acta*, **465**, 549 (1977).

Levin, R. L., E. G. Cravalho, and C. E. Huggins, "The Concentration Polarization Effect in a Multicomponent Electrolyte Solution—The Human Erythrocyte," *J. Theor. Biol.*, **71**, 225 (1978).

Levin, R. L., M. Ushiyama, and E. G. Cravalho, "Water Permeability of Yeast Cells at Sub-Zero Temperatures," *J. Memb. Biol.*, **46**, 91 (1979).

Mansoori, G. A., "Kinetics of Water Loss from Cells at Subzero Centrigrade Temperature," *Cryobiol.*, **12**, 34 (1975).

Mazur, P., "Kinetics of Water Loss from Cells at Subzero Temperatures and the Likelihood of Intracellular Freezing," *J. Gen. Physiol.*, **47**, 347 (1963).

Mazur, P., "Freezing of Living Cells: Mechanisms and Implications," *Am. J. Physiol.*, **143**, C125 (1984).

McGrath, J. J., "Membrane Transport Properties," In *Low Temperature Biotechnology: Emerging Applications and Engineering Contributions*, J. J. McGrath and K. R. Diller, eds., The American Society of Mechanical Engineers, New York, p. 273-330 (1988).

Modell, M., and R. C. Reid, *Thermodynamics and Its Applications*, Prentice-Hall, Englewood Cliffs, NJ (1983).

Morris, G. J., and J. J. McGrath, "Intracellular Ice Nucleation and Gas Bubble Formation in *Spirogyra*," *Cryo-Letters*, **2**, 341 (1981).

Muldrew, K., and L. McGann, "Mechanisms of Intracellular Ice Formation," *Biophys. J.*, **57**, 525 (1990).

Olumide, F., A. Eliashiv, N. Kralios, L. Norton, and B. Eisman, "Hepatic Support with Hepatocyte Suspensions in a Permeable Membrane Dialyzer," *Surgery*, **82**, 599 (1979).

Pitt, R. E., S. P. Myers, T. T. Lin, and P. L. Steponkus, "Subfreezing Volumetric Behavior and Stochastic Modelling of Intracellular Ice Formation in *Drosophila melanogaster* Embryos," *Cryobiol.*, **28**, 72 (1991).

Rich, G. I., R. I. Sha'afi, A. Ramualdez, and A. Solomon, "Effect of Osmolality on the Hydraulic Permeability Coefficient of Red Cells," *J. Gen. Physiol.*, **52**, 941 (1968).

Rubinsky, B., and D. E. Pegg, "A Mathematical Model for the Freezing Process in Biological Tissue," *Proc. R. Soc. Lond.*, **B234**, 343 (1988).

Scheiwe, M. W., and C. Koerber, "Quantitative Cryomicroscopic Analysis of Intracellular Freezing of Granulocytes Without Cryoadditive," *Cryobiol.*, **24**, 473 (1987).

Schwartz, G. J., and K. R. Diller, "Intracellular Freezing of Human Granulocytes," *Cryobiol.*, **21**, 654 (1984).

Seglen, P. O., "Preparation of Rat Liver Cells: III. Enzymatic Requirements for Tissue Dispersion," *Exp. Cell Res.*, **82**, 391 (1973).

Shabana, M., and J. J. McGrath, "Cryomicroscope Investigation and Thermodynamic Modelling of the Freezing of Unfertilized Hamster Ova," *Cryobiol.*, **25**, 338 (1988).

Toner, M., J. Porter, A. Kanai, T. Maki, A. P. Monaco, and E. G. Cravalho, "Comparison of Freezing Behavior of Whole Islets and Single Islet Cells," *Diabetes*, **38**, 280 (1989).

Toner, M., E. G. Cravalho, and M. Karel, "Thermodynamics and Kinetics of Intracellular Ice Formation during Freezing of Biological Cells," *J. Appl. Phys.*, **67**, 1582 (1990a).

Toner, M., E. G. Cravalho, and D. R. Armant, "Water Transport and Estimated Transmembrane Potential during Freezing of Mouse Oocytes," *J. Memb. Biol.*, **115**, 261 (1990b).

Toner, M., E. G. Cravalho, and D. R. Armant, "Cryomicroscopic Analysis of Intracellular Ice Formation during Freezing of Mouse Oocytes," *Cryobiol.*, **28**, 55 (1991).

Toner, M., E. G. Cravalho, and M. Karel, "Cellular Response of Mouse Oocytes to Freezing Stress: Prediction of Intracellular Ice Formation," *J. Biomech. Eng.* 1992 (in press).

Turnbull, D., and J. C. Fisher, "Rate of Nucleation in Condensed Systems," *J. Chem. Phys.*, **17**, 71 (1949).

Turnbull, D., and B. Vonegut, "Nucleation Catalysis," *Ind. Eng. Chem.*, **44**, 1292 (1952).

Uhlmann, D. R., and B. Chalmers, "The Energetics of Nucleation," *Ind. Eng. Chem.*, **57**, 19 (1965).

Yarmush, M. L., M. Toner, J. C. L. Dunn, A. Rotem, A. Hubel, and R. G. Tompkins, "Hepatic Tissue Engineering: Development of Critical Technologies," *Ann. N.Y. Acad. Sci.* 1991 (in press).

Manuscript received Dec. 27, 1991, and revision received May 4, 1992.